Composite Anti-Disturbance Control for Ship Dynamic Positioning Systems with Thruster Faults

Ziwen Yu
Ludong University
Xinjiang Wei (weixinjiang@163.com)
Ludong University https://orcid.org/0000-0001-7475-5658
Huifeng Zhang
Ludong University
Xin Hu
Ludong University
Jian Han
Ludong University

Research Article

Keywords: Anti-disturbance control, Dynamic positioning, DOBC, Fault diagnosis, Stochastic disturbance observer

Posted Date: November 8th, 2021

DOI: https://doi.org/10.21203/rs.3.rs-1023666/v1

Composite anti-disturbance control for ship dynamic positioning systems with thruster faults

Ziwen Yu, Xinjiang Wei*, Huifeng Zhang, Xin Hu, Jian Han

School of Mathematics and Statistics Science, Ludong University, Yantai, China

Abstract

Anti-disturbance control problem is studied for ship dynamic positioning systems with disturbances and thruster faults. The disturbances include slowly-varying environmental disturbances and norm bounded disturbances. For the slowly-varying environmental disturbance, a stochastic disturbance observer is established to give the online estimation. For thruster faults, a fault diagnosis observer is designed. Then, a composite anti-disturbance control (CADC) strategy is raised, which ensures asymptotic mean-square boundedness of the closed-loop system. Finally, the simulation example proves the validity of the controller.
KEY WORDS: Anti-disturbance control; Dynamic positioning; DOBC; Fault diagnosis; Stochastic disturbance observer

1 Introduction

There are various disturbances at sea level. The dynamic positioning(DP) can keep the ship in a predetermined position or track in the presence of external environmental disturbance [1–4]. For unknown constant disturbance, a nonlinear set-point-regulation controller was proposed using a port-Hamiltonian framework [5]. Considering the unknown time-varying disturbance, a PID controller was given based on fuzzy rules [6].

In fact, ships will be affected by different types of disturbances on the sea surface [7, 8]. For multiple disturbances, the composite hierarchical anti-disturbance control(CHADC) strategy was presented, which has advantages of high control precision and strong robustness [9–13]. Considering modeling uncertainty and marine environmental disturbance, a composite control method is raised by combining disturbance observer-based control and H_∞ control [14]. In ref [15], a robust adaptive controller was given for systems with multiple disturbance.

When ships sailing on the sea for a long time, thruster faults will appear inevitably [16, 17]. The faults will degrade system performance, reduce the DP accuracy, and even make the DP system unstable [18–20]. Therefore, it is essential to study the fault diagnosis to improve the reliability of the DP systems [21, 22]. In [23], the asymptotic dynamic positioning for ships with actuator constraints was addressed, whereas the disturbances caused by external environmental is not considered.

In this paper, the DP systems are considered with multiple disturbances and thruster faults. The stochastic disturbance observer and fault diagnosis observer are given to evaluate the disturbance and fault concurrently. Subsequently, a composite anti-disturbance control(CADC) strategy is raised. The main contributions are as follows:

1) The ship dynamic positioning systems with multiple disturbances and thruster faults are considered. In multiple disturbances, the slowly-varying environmental disturbance is considered, which is generated by an external system with white noise.

2) The disturbance observer and fault observer are designed to evaluate the disturbance and fault. Then, the composite controller is given by uniting the disturbance observer-based control with fault-tolerant control.

*Corresponding author. Email: weixinjiang@163.com.

2 Mathematical modeling of ships

Two coordinate frames are defined to mean the ship motion, as represented in the Fig 1. $AXYZ$ is the ship-fixed frame. When the ship is symmetrical left and right, ships center of gravity is origin A. AX is directed from stern to prow, AY is pointed to the starboard, AZ is from top towards bottom. $OX_0Y_0Z_0$ is the north-east-down frame. The OX_0 axis, OY_0 axis and OZ_0 axis points north, east and the center of the earth, respectively. Origin O is considered to be any point on the face of the globe. The dynamic positioning of ship's mathematical model is as below

$$\dot{\eta}(t) = T(\iota)\upsilon, \tag{1}$$

$$A\dot{\upsilon} = -B\upsilon + \tau + \rho(t) + \epsilon(t) + \varepsilon(t), \tag{2}$$

where $\eta = [x, y, \iota]^{\mathrm{T}}$ is the position vector, $\upsilon = [u, v, r]^{\mathrm{T}}$ is the velocity vector, and

$$T(\iota) = \begin{bmatrix} \cos(\iota) & -\sin(\iota) & 0 \\ \sin(\iota) & \cos(\iota) & 0 \\ 0 & 0 & 1 \end{bmatrix}, \tag{3}$$

which satisfies $T^{-1}(\iota) = T^{\mathrm{T}}(\iota)$. $\tau = [\tau_1, \tau_2, \tau_3]^{\mathrm{T}}$ is a three-dimensional column vector, which is formed from

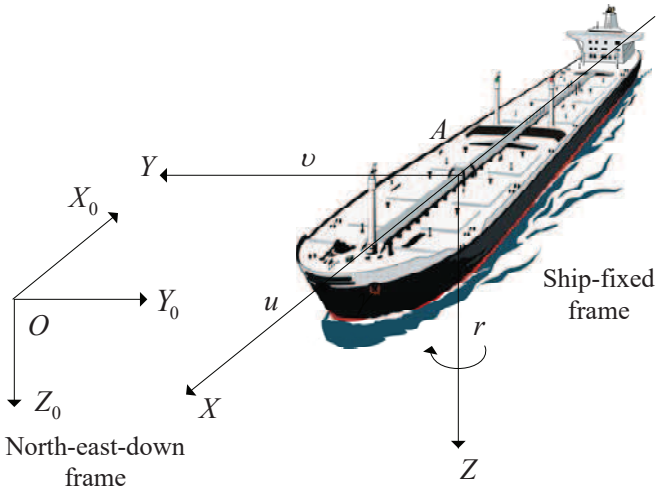

Figure 1: North-east-down and ship-fixed coordinate frames [24].

forces and moments that generated by the propulsion device. $\rho(t)$ is slowly-varying environmental disturbances. $\epsilon(t)$ is the norm bounded disturbance. $\varepsilon(t)$ is a vector that represents the fault caused by the thruster system. A is a inertia matrix, B is a damping matrix.

Based on [25], the yaw angle ι satisfies

$$T(\iota) \approx I. \tag{4}$$

Remark 1: For the ship dynamic positioning systems, the wave-induced yaw ι_w is small enough that $T(\iota) \approx T(\iota + \iota_w)$($\iota_w$ is less than 1° when the vessel sails on the sea and is less than 5° in the severe weather conditions). Considering the yaw angle ι is extremely small, then $cos(\iota + \iota_w) \approx cos(\iota) \approx 1$, $sin(\iota + \iota_w) \approx sin(\iota) \approx 0$ and $T(\iota) \approx I$.

Letting $\mu = \tau$, the DP system is expressed as

$$\dot{X}(t) = GX(t) + H(\mu(t) + \rho(t) + \epsilon(t) + \varepsilon(t)), \tag{5}$$

$$X = \begin{bmatrix} \eta \\ \upsilon \end{bmatrix}, G = \begin{bmatrix} 0 & I \\ 0 & -A^{-1}B \end{bmatrix}, H = \begin{bmatrix} 0 \\ A^{-1} \end{bmatrix},$$

where $X(t) \in \Re^n$, $G \in \Re^{n\times n}$, $H \in \Re^{n\times m}$ and $\mu(t) \in \Re^m$ is the state vector, the coefficient matrix and the control input vector. $\rho(t)$ is slowly-varying environmental disturbances. $\epsilon(t)$ is the norm bounded disturbance, $\varepsilon(t)$ represents the fault caused by the thruster system.

Based on [26], $\rho(t)$ is described as

$$\begin{cases} \rho(t) = T^{-1}(\iota)h(t), \\ \dot{h}(t) = -N^{-1}h(t) + \Theta\zeta(t), \end{cases} \tag{6}$$

where $N \in \Re^{r\times r}$ is the known positive definite diagonal matrices, $h(t)$ represents bias forces and moments, $\Theta \in \Re^{r\times r}$ is the bounded positive definite diagonal matrices, $\zeta(t) \in \Re^r$ is the zero-mean Gauss white noise, and $\|\zeta(t)\|^2 \leq c^*$, c^* is a positive constant.

The fault is indicated as:

$$\dot{\varepsilon}(t) = J\varsigma(t), \tag{7}$$

where J is a known matrix and $\varsigma(t)$ is bounded.

Assumption 1: The pair $(N^{-1}, HT^{-1}(\iota))$ is observable and the pair (G, H) is controllable.

Lemma 1 [27]: For

$$dx(t) = m(x(t), t)dt + n(x(t), t)d\omega(t), t \geq t_0 \geq 0. \tag{8}$$

If $\exists V \in C^{2.1}(\Re^n \times \Re_+)$, $\kappa \in \mathcal{K}_\nu \subset \mathcal{K}_\infty$ and $\psi, s, \theta > 0$, satisfy

$$\kappa(|x|^\psi) \leq V(x, t), \tag{9}$$

$$\mathcal{L}V(x, t) \leq -sV(x, t) + \theta, \tag{10}$$

for $\forall(x, t) \in \Re^n \times \Re_+$. Subsequently

$$\lim_{t\to\infty} \sup E|x(t; t_0, x_0)|^\psi \leq \kappa^{-1}(\frac{\theta}{s}) \tag{11}$$

for $\forall(x, t) \in \Re^n \times \Re_+$. Therefore, the system (8) is asymptotically bounded in pth moment.

According to [28], by replacing $\zeta(t)$ with $\frac{d\omega(t)}{dt}$, the DP systems can be depicted by:

$$dX(t) = GX(t)dt + H(\mu(t) + \rho(t) + \epsilon(t) + \varepsilon(t))dt, \tag{12}$$

$$\begin{cases} \rho(t) = T^{-1}(\iota)h(t), \\ dh(t) = -N^{-1}h(t)dt + \Theta d\omega(t), \end{cases} \tag{13}$$

based on [29, 30], $\omega(t)$ is an independent standard Wiener process.

3 Main results

Supposing $X(t)$ is available. The composite observer consisting of SDO and FDO is devised to estimate $\rho(t)$ and $\varepsilon(t)$. After that, the CADC strategy is proposed.

3.1 Composite observer

3.1.1 Stochastic disturbance observer (SDO)

The SDO is given as

$$\begin{cases} \hat{\rho}(t) = T^{-1}(\iota)\hat{h}(t), \\ \hat{h}(t) = q(t) + L_1 X(t), \\ dq(t) = (-N^{-1} - L_1 H T^{-1}(\iota))(q(t) + L_1 X(t))dt - L_1 G X(t)dt - L_1 H(\mu(t) + \hat{\varepsilon}(t))dt, \end{cases} \tag{14}$$

where $\hat{\rho}(t)$ is evaluation of $\rho(t)$, $p(t)$ is the auxiliary variable of SDO (14), and the observer gain L_1 can be determined by the method of pole placement.

Letting $e_h(t) = h(t) - \hat{h}(t)$, the error systems is

$$de_h(t) = (-N^{-1} - L_1 H T^{-1}(\iota))e_h(t)dt - L_1 H e_\varepsilon(t)dt - L_1 H \epsilon(t)dt + \Theta d\omega(t). \tag{15}$$

3.1.2 Fault diagnosis observer (FDO)

The FDO is expressed as

$$\begin{cases} \hat{\varepsilon}(t) = p(t) - L_2 X(t), \\ dp(t) = L_2 H(p(t) - L_2 X(t))dt + L_2(GX(t) + H\mu(t) + H\hat{\rho}(t))dt, \end{cases} \tag{16}$$

where $\hat{\varepsilon}(t)$ is the evaluation of $\varepsilon(t)$, $p(t)$ is the middle variable of FDO, the gain L_2 of the observer(16) satisfies

$$L_2 H = D. \tag{17}$$

Assuming D is a Hurwitz matrix. Denoting $e_\varepsilon(t) = \varepsilon(t) - \hat{\varepsilon}(t)$, then

$$de_\varepsilon(t) = J\varsigma(t)dt + L_2 H e_\varepsilon(t)dt + L_2 H T^{-1}(\iota)e_h(t)dt + L_2 H \epsilon(t)dt. \tag{18}$$

3.2 Composite anti-disturbance control (CADC)

The CADC strategy is put forward by using H_∞ technique and toolbox of LMI, hence the system (12) is asymptotically mean-square bounded.

On account of the SDO (14) and FDO (16), the composite controller is devised as follows

$$\mu(t) = KX(t) - \hat{\rho}(t) - \hat{\varepsilon}(t), \tag{19}$$

where K is coefficient matrix, which can be derived using the LMI.

On the basis of (12) and (19), one has

$$dX(t) = (G + HK)X(t)dt + HT^{-1}(\iota)e_h(t)dt + He_\varepsilon(t)dt + H\epsilon(t)dt. \tag{20}$$

Combining (15), (18) and (20), then

$$d\aleph(t) = \bar{G}\chi(t)dt + \bar{H}\epsilon(t)dt + \bar{J}\varsigma(t)dt + \bar{\Theta}d\omega(t), \tag{21}$$

$$\varpi(t) = C\chi(t), \tag{22}$$

where

$$\bar{G}=\begin{bmatrix} G+HK & HT^{-1}(\iota) & H \\ 0 & -N^{-1}-L_1HT^{-1}(\iota) & -L_1H \\ 0 & L_2HT^{-1}(\iota) & L_2H \end{bmatrix}, \bar{H}=\begin{bmatrix} H \\ -L_1H \\ L_2H \end{bmatrix},$$
$$\bar{J}=\begin{bmatrix} 0 \\ 0 \\ J \end{bmatrix}, \bar{\Theta}=\begin{bmatrix} 0 \\ \Theta \\ 0 \end{bmatrix}, C=\begin{bmatrix} C_1 & C_2 & C_3 \end{bmatrix}, \aleph(t)=\begin{bmatrix} X(t) \\ e_h(t) \\ e_\varepsilon(t) \end{bmatrix}.$$

Then, the following results through the stability analysis of the system (21).

Theorem 1: Under Assumption 1, consider system (12) with multiple disturbances and thruster faults, if $\exists Q_1>0$, $Q_2>0$, $Q_3>0$, constant $\gamma>0$ and matrix R_1, satisfying

$$\Omega=\begin{bmatrix} \Pi_{11} & \Pi_{12} & HQ_3 & H & 0 & Q_1C_1^{\mathrm{T}} \\ * & \Pi_{22} & \Pi_{23} & -L_1H & 0 & Q_2C_2^{\mathrm{T}} \\ * & * & \Pi_{33} & L_2H & J & Q_3C_3^{\mathrm{T}} \\ * & * & * & -\gamma^2I & 0 & 0 \\ * & * & * & * & -\gamma^2I & 0 \\ * & * & * & * & * & -I \end{bmatrix}<0, \tag{23}$$

where

$$\begin{aligned} \Pi_{11}&=GQ_1+Q_1G^{\mathrm{T}}+HR_1+R_1^{\mathrm{T}}H^{\mathrm{T}}, \\ \Pi_{12}&=HT^{-1}(\iota)Q_2, \\ \Pi_{22}&=-N^{-1}Q_2-Q_2N^{-1}-L_1HT^{-1}(\iota)Q_2-Q_2T(\iota)H^{\mathrm{T}}L_1^{\mathrm{T}}, \\ \Pi_{23}&=-L_1HQ_3+Q_2T(\iota)H^{\mathrm{T}}L_2^{\mathrm{T}}, \\ \Pi_{33}&=L_2HQ_3+Q_3H^{\mathrm{T}}L_2^{\mathrm{T}}. \end{aligned}$$

By adjusting the gain L_1 of SDO (15), the gain L_2 of FDO (18) and solving the gain K of the controller (19) with $K=R_1Q_1^{-1}$, then all states of system (21) are asymptotically mean-square bounded. In the meantime, $\|\varpi(t)\|<\gamma(\|\epsilon(t)\|+\|\varsigma(t)\|)$ for $\forall\epsilon(t),\varsigma(t)\in L_2(0,T]$.

Proof:(i) For the system (21) with $\epsilon(t)=\varsigma(t)=0$, selecting

$$V(\aleph(t),t)=\aleph^{\mathrm{T}}(t)\Psi\aleph(t), \tag{24}$$

and

$$\Psi=\begin{bmatrix} \Psi_1 & 0 & 0 \\ 0 & \Psi_2 & 0 \\ 0 & 0 & \Psi_3 \end{bmatrix}=\begin{bmatrix} Q_1^{-1} & 0 & 0 \\ 0 & Q_2^{-1} & 0 \\ 0 & 0 & Q_3^{-1} \end{bmatrix}>0. \tag{25}$$

the derivative of (24) is

$$\begin{aligned} \mathcal{L}V(\aleph(t),t) &= \frac{\partial V}{\partial\aleph}\left(\bar{G}\aleph(t)\right)+Tr(\bar{\Theta}^{\mathrm{T}}\Psi\bar{\Theta}) \\ &=\aleph^{\mathrm{T}}(t)\left(\Psi\bar{G}+\bar{G}^{\mathrm{T}}\Psi\right)\aleph(t)+Tr(\bar{\Theta}^{\mathrm{T}}\Psi\bar{\Theta}) \\ &=\aleph^{\mathrm{T}}(t)\Xi_0\aleph(t)+\alpha(t), \end{aligned} \tag{26}$$

where

$$\Omega_0=\Psi\bar{G}+\bar{G}^{\mathrm{T}}\Psi,\ \ \alpha(t)=Tr(\bar{\Theta}^{\mathrm{T}}\Psi\bar{\Theta}).$$

Since $\bar{\Theta}$ and Ψ are bounded, for (26), $\exists\,\imath>0$, such that $0<\alpha(t)<\imath$, which implies that

$$\mathcal{L}V(\aleph(t),t)=\aleph^{\mathrm{T}}(t)\Xi_0\aleph(t)+r(t)\leq\aleph^{\mathrm{T}}(t)\Xi_0\aleph(t)+\imath. \tag{27}$$

When $\Xi_0 < 0$, $\exists \nu > 0$, one has

$$\Xi_0 < 0 \Rightarrow \Xi_0 + \nu I < 0. \tag{28}$$

Based on (24), (26), (27) and (28), choosing $\kappa = \lambda_{min}(\Psi)|\aleph|^p$, $\vartheta = \frac{\theta}{\lambda_{max}(\Psi)}$ and $p = 2$, the following inequalities hold

$$\kappa(|\aleph|^p) = \lambda_{min}(\Psi)|\aleph|^2 \leq \aleph^{\mathrm{T}}(t)\Psi\aleph(t) = V(\aleph(t), t), \tag{29}$$

$$\mathcal{L}V(\aleph(t), t) \leq -\vartheta V(\aleph(t)) + \imath. \tag{30}$$

Subsequently,

$$EV(\aleph(t), t) \leq V(\aleph(0))e^{-\vartheta t} + \frac{\imath}{\theta} \tag{31}$$

and

$$\lim_{t\to\infty} \sup E|\aleph(t; t_0, \aleph_0)|^p \leq \frac{\imath}{\vartheta\lambda_{max}(\Psi)} = \frac{\imath}{\theta}. \tag{32}$$

In the light of Lemma 1, system (21) is asymptotically mean-square bounded under $\epsilon(t) = \varsigma(t) = 0$.

(ii) For the case of $\epsilon(t), \varsigma(t) \in L_2(0, T]$, choosing

$$W(t) = E\int_0^t \left[\varpi^{\mathrm{T}}(s)\varpi(s) - \gamma^2(\epsilon^{\mathrm{T}}(s)\epsilon(s) + \varsigma^{\mathrm{T}}(s)\varsigma(s)) + \mathcal{L}V(\aleph(s), s)\right] ds.$$

Considering (29), then

$$\begin{aligned} W(t) &= E\int_0^t \left[\varpi^{\mathrm{T}}(s)\varpi(s) - \gamma^2(\epsilon^{\mathrm{T}}(s)\epsilon(s) + \varsigma^{\mathrm{T}}(s)\varsigma(s)) + \mathcal{L}V(\aleph(s), s)\right] ds \\ &\leq E\int_0^t \left[\varpi^{\mathrm{T}}(s)\varpi(s) - \gamma^2(\epsilon^{\mathrm{T}}(s)\epsilon(s) + \varsigma^{\mathrm{T}}(s)\varsigma(s)) + \aleph^{\mathrm{T}}(s)\Omega_0\aleph(s)\right] ds + \imath \\ &= E\int_0^t \begin{bmatrix} \aleph(s) \\ \epsilon(s) \\ \varsigma(s) \end{bmatrix}^{\mathrm{T}} \Xi_1 \begin{bmatrix} \aleph(s) \\ \epsilon(s) \\ \varsigma(s) \end{bmatrix} ds + \imath \\ &= W_1(t) + \imath, \end{aligned} \tag{33}$$

where

$$W_1(t) = E\int_0^t \begin{bmatrix} \aleph(s) \\ \epsilon(s) \\ \varsigma(s) \end{bmatrix}^{\mathrm{T}} \Xi_1 \begin{bmatrix} \aleph(s) \\ \epsilon(s) \\ \varsigma(s) \end{bmatrix} ds, \quad \Xi_1 = \begin{bmatrix} \Xi_0 + C^{\mathrm{T}}C & \Psi\bar{H} & \Psi\bar{J} \\ \bar{H}^{\mathrm{T}}\Psi & -\gamma^2 I & 0 \\ \bar{J}^{\mathrm{T}}\Psi & 0 & -\gamma^2 I \end{bmatrix}. \tag{34}$$

Our main results are as follows:

1): $\Xi_1 < 0 \Leftrightarrow \Xi_2 < 0$. Considering (21), (24), (34) and Schur complement lemma, $\Xi_1 < 0 \Leftrightarrow \Xi_2 < 0$, where

$$\Xi_2 = \begin{bmatrix} \Lambda_{11} & \Lambda_{12} & \Psi_1 H & \Psi_1 H & 0 & C_1^{\mathrm{T}} \\ * & \Lambda_{22} & \Lambda_{23} & -\Psi_2 L_1 H & 0 & C_2^{\mathrm{T}} \\ * & * & \Lambda_{33} & \Psi_3 L_2 H & \Psi_3 J & C_3^{\mathrm{T}} \\ * & * & * & -\gamma^2 I & 0 & 0 \\ * & * & * & * & -\gamma^2 I & 0 \\ * & * & * & * & * & -I \end{bmatrix}, \tag{35}$$

with

$$\begin{aligned}
\Lambda_{11} &= \Psi_1 G + G^{\mathrm{T}}\Psi_1 + \Psi_1 HK + K^{\mathrm{T}}H^{\mathrm{T}}\Psi_1,\\
\Lambda_{12} &= \Psi_1 HT^{-1}(\iota),\\
\Lambda_{22} &= -\Psi_2 N^{-1} - N^{-1}\Psi_2 - \Psi_2 L_1 HT^{-1}(\iota) - T(\iota)H^{\mathrm{T}}L_1^{\mathrm{T}}\Psi_2,\\
\Lambda_{23} &= -\Psi_2 L_1 H + T(\iota)H^{\mathrm{T}}L_2^{\mathrm{T}}\Psi_3,\\
\Lambda_{33} &= \Psi_3 L_2 H + H^{\mathrm{T}}L_2^{\mathrm{T}}\Psi_3.
\end{aligned}$$

2): $\Xi_2 < 0 \Leftrightarrow \Xi_3 < 0$. Multiplied by $diag\{Q_1, Q_2, Q_3, I, I, I\}$ on both sides of the matrix Ξ_2 is adopted, yields

$$\Xi_3 = \begin{bmatrix}
\Pi_{11} & \Pi_{12} & HQ_3 & H & 0 & Q_1 C_1^{\mathrm{T}}\\
* & \Pi_{22} & \Pi_{23} & -L_1 H & 0 & Q_2 C_2^{\mathrm{T}}\\
* & * & \Pi_{33} & L_2 H & J & Q_3 C_3^{\mathrm{T}}\\
* & * & * & -\gamma^2 I & 0 & 0\\
* & * & * & * & -\gamma^2 I & 0\\
* & * & * & * & * & -I
\end{bmatrix} < 0, \tag{36}$$

here

$$\begin{aligned}
\Pi_{11} &= GQ_1 + Q_1 G^{\mathrm{T}} + HKQ_1 + Q_1 K^{\mathrm{T}}H^{\mathrm{T}},\\
\Pi_{12} &= HT^{-1}(\iota)Q_2,\\
\Pi_{22} &= -N^{-1}Q_2 - Q_2 N^{-1} - L_1 HT^{-1}(\iota)Q_2 - Q_2 T(\iota)H^{\mathrm{T}}L_1^{\mathrm{T}},\\
\Pi_{23} &= -L_1 HQ_3 + Q_2 T(\iota)H^{\mathrm{T}}L_2^{\mathrm{T}},\\
\Pi_{33} &= L_2 HQ_3 + Q_3 H^{\mathrm{T}}L_2^{\mathrm{T}}.
\end{aligned}$$

3): $\Xi_3 < 0 \Leftrightarrow \Xi < 0$. For $\Xi_3 < 0$, choosing $K = R_1 Q_1^{-1}$, we have $\Xi < 0$.

So, one has $\Xi < 0 \Leftrightarrow \Xi_3 < 0 \Leftrightarrow \Xi_2 < 0 \Leftrightarrow \Xi_1 < 0$, which means that $\Xi_0 < 0$ and $W_1(t) < 0$ hold. From (33), we have $W(t)$ is bounded, then $\|\varpi(t)\| < \gamma(\|\epsilon(t)\| + \|\varsigma(t)\|)$.

4 Simulation examples

Taking Cybership II with width of 0.29 m, length of 1.255 m and scale of 1:70 as an example [31].

4.1 Disturbance case 1: $\Theta = diag\{3, 2.3, 2.6\}$

The coefficient matrices are taken as follows:

$$A = \begin{bmatrix} 25.8 & 0 & 0\\ 0 & 33.8 & 1.0948\\ 0 & 1.0948 & 2.76 \end{bmatrix}, B = \begin{bmatrix} 0.72253 & 0 & 0\\ 0 & 0.88965 & 7.25\\ 0 & -0.03130 & 1.9 \end{bmatrix}.$$

Selecting $\eta_0 = [1\ m, 1\ m, \pi/4\ rad]^{\mathrm{T}}$ and $\upsilon_0 = [0\ m/s, 0\ m/s, 0\ rad/s]^{\mathrm{T}}$, then $X(0) = [1, 1, \pi/4, 0, 0, 0]^{\mathrm{T}}$. Assuming the bound of $\epsilon(t)$ is 1 and the thruster fault is

$$\varepsilon(t) = \begin{bmatrix} 10 - 10sin(0.001t + 1)\ 10 - 10sin(0.001t + 2)\ 10 - 10sin(0.001t + 3) \end{bmatrix}^{\mathrm{T}}.$$

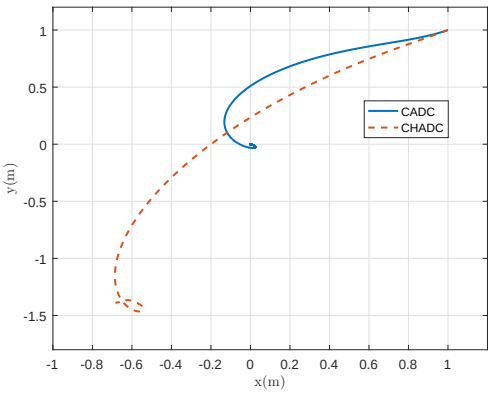

(a) Trajectory of the ship in plan-xy.

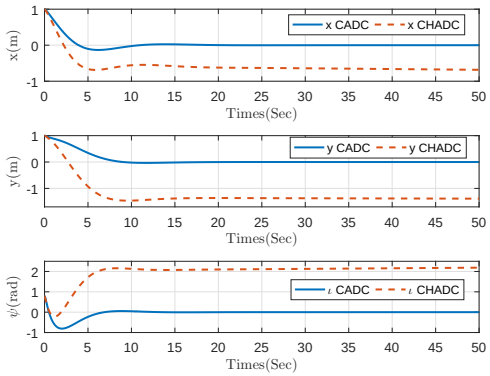

(b) Responses of ship position.

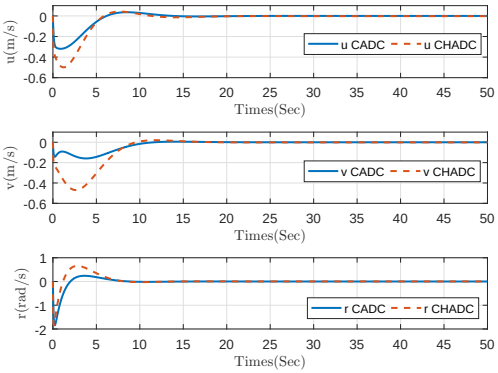

(c) Responses of ship velocity.

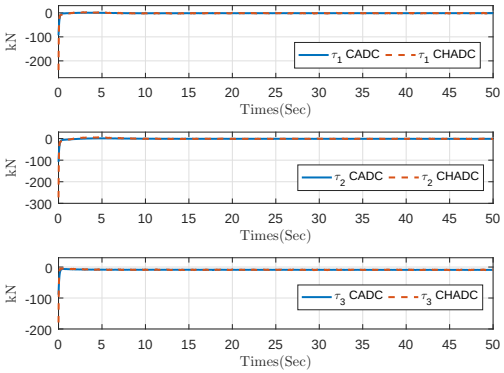

(d) Curves of the control input.

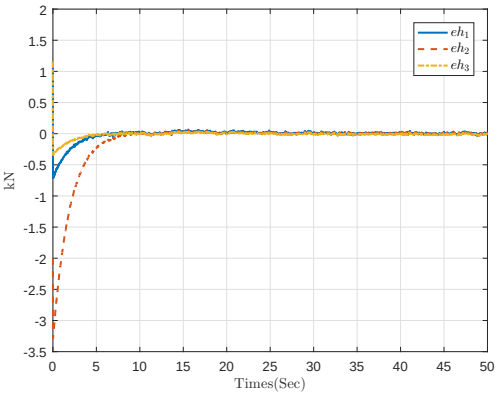

(e) Curves of the disturbance estimation error.

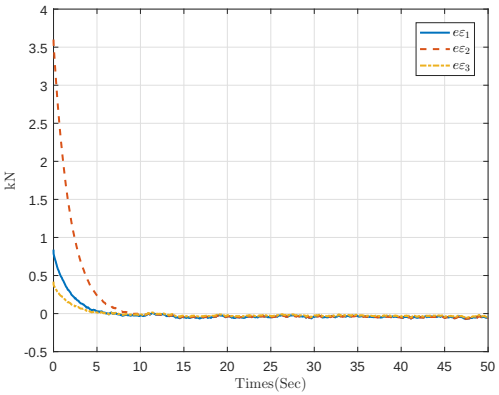

(f) Curves of the fault estimation error.

Figure 2: Contrastive curves of disturbance case 1.

Selecting the output as $\varpi(t) = C\chi(t)$, $\gamma = 10$ and $C_1 = [1,1,1,1,1,1]$, $C_2 = [0,0,0]$, $C_3 = [0,0,0]$, the parameters of disturbance (6) are

$$N = \begin{bmatrix} 0.05 & 0 & 0 \\ 0 & 0.05 & 0 \\ 0 & 0 & 0.05 \end{bmatrix}, \Theta = \begin{bmatrix} 3 & 0 & 0 \\ 0 & 2.3 & 0 \\ 0 & 0 & 2.6 \end{bmatrix}.$$

By placing the poles of $-N^{-1} - L_1 H T^{-1}(\iota)$ at $[-300\ -300\ -300]$, the observation gain L_1 can be obtained

$$L_1 = \begin{bmatrix} 0\,0\,0 & 7224.0000 & 0 & 0 \\ 0\,0\,0 & 0 & 9464.0000 & 306.5440 \\ 0\,0\,0 & 0 & 306.5440 & 772.8000 \end{bmatrix}.$$

Based on (18), choosing $S = diag\{-8,-8,-8\}$, the fault observation gain L_2 can be obtained that

$$L_2 = \begin{bmatrix} 0\,0\,0 & -206.4000 & 0 & 0 \\ 0\,0\,0 & 0 & -270.4000 & -8.7584 \\ 0\,0\,0 & 0 & -8.7584 & -22.0800 \end{bmatrix}.$$

Based on Theorem 1, one has

$$Q_1 = \begin{bmatrix} 308.1337 & -96.6093 & -73.5695 & -95.3816 & 12.7475 & -51.0975 \\ -96.6093 & 295.0344 & -66.7552 & 4.0045 & -86.8390 & -44.3572 \\ -73.5696 & -66.7552 & 302.7190 & 23.5956 & -10.4535 & -171.8649 \\ -95.3816 & 4.0045 & 23.5956 & 59.1977 & -1.3900 & 9.4624 \\ 12.7475 & -86.8390 & -10.4535 & -1.3900 & 50.5828 & 33.7809 \\ -51.0975 & -44.3572 & -171.8649 & 9.4624 & 33.7809 & 231.2220 \end{bmatrix},$$

$$Q_2 = \begin{bmatrix} 36.9780 & 0 & -0.0001 \\ 0 & 36.9785 & 0 \\ -0.0001 & 0 & 36.9679 \end{bmatrix}, Q_3 = \begin{bmatrix} 3.9564 & 0 & 0 \\ 0 & 3.9565 & 0.0001 \\ 0 & -0.0001 & 3.9540 \end{bmatrix},$$

$$R_1 = \begin{bmatrix} -120.2714 & -16.0909 & -3.6584 & -384.2185 & -18.9038 & -1.7369 \\ -24.1237 & -116.8468 & -59.3510 & -14.0846 & -389.1557 & -2.5195 \\ -42.1946 & -36.2377 & -195.7416 & -10.6494 & 24.0253 & -250.8027 \end{bmatrix}.$$

$$K = \begin{bmatrix} -35.6227 & -33.0368 & -30.6078 & -45.5143 & -35.7308 & -29.8851 \\ -36.9426 & -41.7950 & -36.2603 & -38.4792 & -56.4309 & -33.3255 \\ -28.9634 & -28.8859 & -29.6037 & -29.0398 & -28.9565 & -29.6120 \end{bmatrix},$$

4.2 Disturbance case 2: $\Theta = 5 \times diag\{3, 2.3, 2.6\}$

The initial values and design control parameters are the same as case 1, the parameters of the disturbances (6) are given by

$$N = \begin{bmatrix} 0.05 & 0 & 0 \\ 0 & 0.05 & 0 \\ 0 & 0 & 0.05 \end{bmatrix}, \Theta = 5 \times \begin{bmatrix} 3 & 0 & 0 \\ 0 & 2.3 & 0 \\ 0 & 0 & 2.6 \end{bmatrix}.$$

In Fig 2-3, (a) is the ship's trajectory from initial position $(1\ m, 1\ m)$. The curves of ship position are illustrated in (b). (c) represents the responses of ship velocity. The control input can be seen in (d). (e)-(f) show the curves of estimation errors for the disturbances and faults.

In Fig 2(a) and 3(a), it is shown that the CADC can make the ship stay in desired position $(0\ m, 0\ m)$ and maintain a fixed attitude steadily compared with [14]. In (b)-(c) of Fig 2-3, we know that the CADC scheme presented in this paper can make the states of DP ship asymptotically mean-square bounded. As can be seen from Fig 2(e)-(f) and 3(e)-(f), the estimation errors of disturbances and faults are satisfactory.

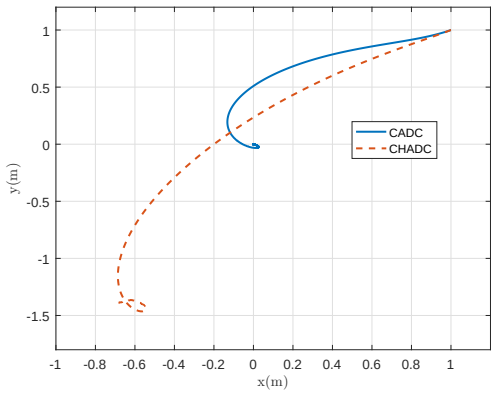

(a) Trajectory of the ship in plan-xy.

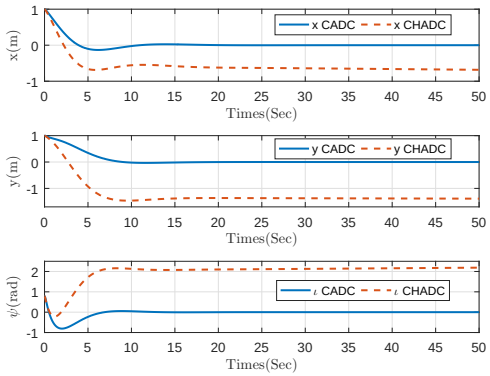

(b) Responses of ship position.

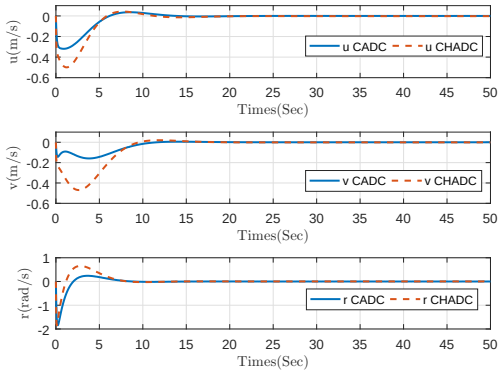

(c) Responses of ship velocity.

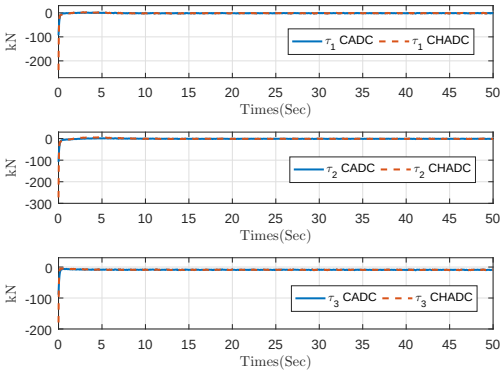

(d) Curves of the control input.

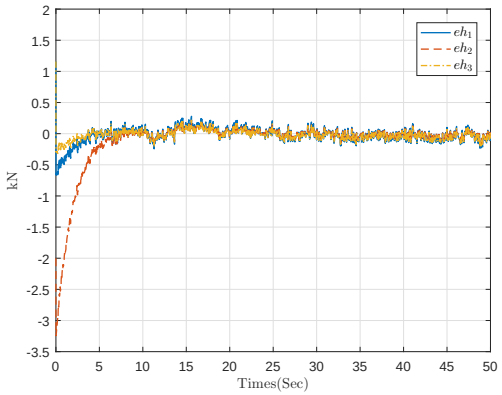

(e) Curves of the disturbance estimation error.

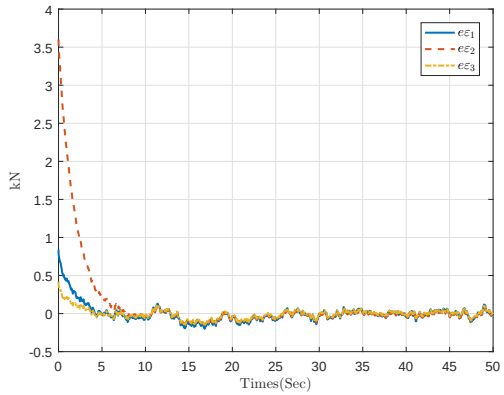

(f) Curves of the fault estimation error.

Figure 3: Comparison curves of disturbance case 2.

5 Conclusions

For the ship dynamic positioning systems with multiple disturbances and thruster faults, a composite observer including SDO and FDO is raised to evaluate the disturbances and faults simultaneously. Based on the estimation, the CADC strategy is put forward by using disturbance observer-based control, H_∞ control and fault-tolerant control. In this paper, the signal thruster fault is considered. The next work in the future is the anti-disturbance control for the ship dynamic positioning systems with multiple disturbances and multiple faults.

Acknowledgements This work was proposed by the National Natural Science Foundation of China 61973149 and the Key project of Natural Science Foundation of Shandong Province ZR2020KF029.

Data Availability Statement The experimental data of the DP model can be found in [31], respectively. The code of this paper is not available.

Compliance with ethical standards

Conflict of interest No conflict of interest exits in this submission, and the manuscript has been approved by all authors for publication. I would like to declare on behalf of my co-authors that this work is the original research that has not been published previously, and not under consideration for publication elsewhere, in whole or in part.

References

[1] Sørensen AJ (2011) A survey of dynamic positioning control systems. *Annual Reviews in Control* 35(1): 123-136.

[2] Fossen TI (1994) *Guidance and Control of Ocean Vehicles.* Chichester, UK: John Wiley & Sons, Inc.

[3] Saelid S, Jenssen NA and Balchen JG (1983) Design and analysis of a dynamic positioning system based on the Kalman filtering and optimal control. *IEEE Transactions on Automatic Control* 28(3): 331-339.

[4] Zhang GQ, Huang CF, Zhang XK and Zhang WD (2018) Practical constrained dynamic positioning control for uncertain ship through the minimal learning parameter technique. *IET Control Theory and Applications* 12(18): 2526-2533.

[5] Donaire A and Perez T (2012) Dynamic positioning of marine craft using a port-Hamiltonian framework. *Automatica* 48(5): 851-856.

[6] Xu SW, Wang XF, Yang JM and Wang L (2019) A fuzzy rule based PID controller for dynamic positioning of vessels in variable environmental disturbances. *Journal of Marine Science and Technology* 25(3): 914-924.

[7] Gao ZY and Guo G (2020) Command filtered path tracking control of saturated ASVs based on time-varying disturbance observer. *Asian Journal of Control* 22(3): 1197-1210.

[8] Xie W, Reis J, Cabecinhas D and Silvestre C (2020) Design and experimental validation of a nonlinear controller for underactuated surface vessels. *Nonlinear Dynamics* 102(4): 2563-2581.

[9] Wei XJ, Chen N, Deng CH, Liu XH and Tang MQ (2012) Composite stratified anti-disturbance control for a class of MIMO discretełtime systems with nonlinearity. *International Journal of Robust and Nonlinear Control* 22(4): 453-472.

[10] Wei XJ, Dong LW, Zhang HF, Han J and Hu X (2020) Composite anti-disturbance control for stochastic systems with multiple heterogeneous disturbances and input saturation. *ISA Transactions* 100: 436-445.

[11] Zhang HF, Wei XJ, Karimi HR and Han J (2018) Anti-disturbance control based on disturbance observer for nonlinear systems with bounded disturbances. *Journal of the Franklin Institute-Engineering and Applied Mathematics* 355(12): 4916-4930.

[12] Sun SX, Wei XJ, Zhang HF, Karimi HR and Han J (2018) Composite fault-tolerant control with disturbance observer for stochastic systems with multiple disturbances. *Journal of the Franklin Institute-Engineering and Applied Mathematics* 355(12): 4897-4915.

[13] Zhang HF, Wei XJ, Zhang LY and Tang MQ (2017) Disturbance rejection for nonlinear systems with mismatched disturbances based on disturbance observer. *Journal of the Franklin Institute-Engineering and Applied Mathematics* 354(11): 4404-4424.

[14] Hu X, Wei XJ, Zhang HF, Xie WB and Zhang Q (2020) Composite anti-disturbance dynamic positioning of vessels with modelling uncertainties and disturbances. *Applied Ocean Research* 105: 102404.

[15] Du JL, Hu X, Krstić, M and Sun YQ (2018) Dynamic positioning of ships with unknown parameters and disturbances. *Control Engineering Practice* 76: 22-30.

[16] Lin YY and Du JL (2016) Fault-Tolerant Control for Dynamic Positioning of Ships Based on an Iterative Learning. *Proceedings of the 35th Chinese Control Conference* 1116-1122.

[17] Dong HR, Lin X, Yao XM, Bai WQ and Ning B (2018) Composite Disturbance-Observer-Based Control and H Control for High Speed Trains with Actuator Faults. *Asian Journal of Control* 20(2): 735-745.

[18] Han J, Liu XH, Wei XJ, Hu X and Zhang HF (2019) Reduced-order observer based fault estimation and fault-tolerant control for switched stochastic systems with actuator and sensor faults. *ISA Transactions* 88: 91-101.

[19] Silva AA, Gupta S, Bazzi AM and Ulatowski A (2018) Wavelet-based information filtering for fault diagnosis of electric drive systems in electric ships. *ISA Transactions* 78: 105-115.

[20] Choi K, Kim Y, Kim SK and Kim KS (2021) Current and Position Sensor Fault Diagnosis Algorithm for PMSM Drives Based on Robust State Observer. *IEEE Transactions on Industrial Electronics* 68(6): 5227-5236.

[21] Xie WB, Guo MH, Xu BL and Wang X (2021) Fault tolerant robust control with transients for over-actuated nonlinear systems. *Nonlinear Dynamics* 104(3): 2433-2450.

[22] Xia KW and Zou Y (2020) Adaptive fixed-time fault-tolerant control for noncooperative spacecraft proximity using relative motion information. *Nonlinear Dynamics* 100(3): 2521-2535.

[23] Su YX, Zheng CH and Mercorelli P (2017) Nonlinear PD Fault-Tolerant Control for Dynamic Positioning of Ships with Actuator Constraints. *IEEE-ASME Transactions on Mechatronics* 22(3): 1132-1142.

[24] Fossen TI (2011) *Handbook of marine craft hydrodynamics and motion control.* Chichester, UK: John Wiley & Sons, Ltd.

[25] Wang YL and Han QL (2018) Network-based modelling and dynamic output feedback control for unmanned marine vehicles in network environments. *Automatica* 91: 43-53.

[26] Fossen TI and Strand JP (1999) Passive nonlinear observer design for ships using Lyapunov methods: full-scale experiments with a supply vessel. *Automatica* 35: 3-16.

[27] Mao XR and Yuan CG (2006) *Stochastic differential equations with Markovian switching.* London: Imperial College Press.

[28] Øksendal B (2003) *Stochastic Differential Equations: An Introduction with Applications.* 6th edition. New York: Springer-Verlag.

[29] Hu F (2017) The modulus of continuity theorem for G-Brownian motion. *Communications in Statistics Theory and Methods* 46(7): 3586-3598.

[30] Hu F, Chen ZJ and Zhang DF (2014) How big are the increments of G-brownian motion? *Science China Mathematics* 57(8): 1687-1700.

[31] Skjetne R, Øyvind S and Fossen TI (2004) Modeling, identification, and adaptive maneuvering of CyberShip II: A complete design with experiments. *IFAC Proceedings Volumes* 37(10): 203-208.